The Astrophysical Journal, 581:981–987, 2002 December 20

THE FAINT OPTICAL AFTERGLOW AND HOST GALAXY OF GRB 020124: IMPLICATIONS FOR THE NATURE OF DARK GAMMA-RAY BURSTS

E. Berger,[1] S. R. Kulkarni,[1] J. S. Bloom,[1] P. A. Price,[1,2] D. W. Fox,[1] D. A. Frail,[1,3] T. S. Axelrod,[2] R. A. Chevalier,[4] E. Colbert,[5] E. Costa,[6] S. G. Djorgovski,[1] F. Frontera,[7,8] T. J. Galama,[1] J. P. Halpern,[9] F. A. Harrison,[1] J. Holtzman,[10] K. Hurley,[11] R. A. Kimble,[12] P. J. McCarthy,[13] L. Piro,[6] D. Reichart,[1] G. R. Ricker,[14] R. Sari,[15] B. P. Schmidt,[2] J. C. Wheeler,[16] R. Vanderppek,[14] and S. A. Yost[1]

Received 2002 July 15; accepted 2002 August 20

ABSTRACT

We present ground-based optical observations of GRB 020124 starting 1.6 hr after the burst, as well as subsequent Very Large Array and *Hubble Space Telescope* (*HST*) observations. The optical afterglow of GRB 020124 is one of the faintest afterglows detected to date, and it exhibits a relatively rapid decay, $F_\nu \propto t^{-1.60\pm0.04}$, followed by further steepening. In addition, a weak radio source was found coincident with the optical afterglow. The *HST* observations reveal that a positionally coincident host galaxy must be the faintest host to date, $R \gtrsim 29.5$ mag. The afterglow observations can be explained by several models requiring little or no extinction within the host galaxy, $A_V^{\rm host} \approx 0$–0.9 mag. These observations have significant implications for the interpretation of the so-called dark bursts (bursts for which no optical afterglow is detected), which are usually attributed to dust extinction within the host galaxy. The faintness and relatively rapid decay of the afterglow of GRB 020124, combined with the low inferred extinction, indicate that some dark bursts are intrinsically dim and not dust obscured. Thus, the diversity in the underlying properties of optical afterglows must be observationally determined before substantive inferences can be drawn from the statistics of dark bursts.

Subject headings: cosmology: observations — dust, extinction — gamma rays: bursts

1. INTRODUCTION

One of the main observational results stemming from 5 yr of gamma-ray burst (GRB) follow-ups at optical wavelengths is that about 60% of well-localized GRBs lack a detected optical afterglow ("dark bursts": Taylor et al. 2000; Fynbo et al. 2001; Lazzati, Covino, & Ghisellini 2002; Reichart & Yost 2001). In some cases, a nondetection of the optical afterglow could simply be due to a failure to image quickly and/or deeply enough. However, there are two GRBs for which there is strong evidence that the optical emission should have been detected, based on an extrapolation of the radio and X-ray emission (Djorgovski et al. 2001a; Piro et al. 2002). One interpretation in these two cases is that the optical light was extinguished by dust, either within the immediate environment of the burst or elsewhere along the line of sight (e.g., Groot et al. 1998). An alternative explanation is a high redshift, leading to absorption of the optical light in the Lyα forest. However, the redshifts of the underlying host galaxies of these GRBs are of order unity (Djorgovski et al. 2001a; Piro et al. 2002).

Several authors have recently argued that a large fraction of the dark bursts are due to dust extinction within the local environment of the bursts (e.g., Lazzati et al. 2002; Reichart & Price 2002; Reichart & Yost 2001), but other scenarios have also been suggested (e.g., Lazzati et al. 2002). Moreover, it has been noted that regardless of the location of extinction within the host galaxy, the fraction of dark bursts is a useful upper limit on the fraction of obscured star formation (Kulkarni et al. 2000; Djorgovski et al. 2001b; Ramirez-Ruiz, Trentham, & Blain 2002; Reichart & Price 2002).

However, from an observational point of view, we must have a clear understanding of the diversity of afterglow properties before extracting astrophysically interesting inferences from dark bursts. For example, afterglows that are intrinsically faint or fade rapidly (relative to the detected population) would certainly bias the determination of the fraction of truly obscured bursts. In this vein, Fynbo et al. (2001), noting the faint optical afterglow of GRB 000630, argue that some dark bursts are due to a failure to image deeply and/or quickly enough, rather than to dust extinction. Observations of the faint afterglow of GRB 980613 (Hjorth et al. 2002) point to the same conclusion.

[1] Division of Physics, Mathematics, and Astronomy, 105-24, California Institute of Technology, Pasadena, CA 91125.
[2] Research School of Astronomy and Astrophysics, Mount Stromlo Observatory, via Cotter Road, Weston Creek 2611, Australia.
[3] National Radio Astronomy Observatory, Socorro, NM 87801.
[4] Department of Astronomy, University of Virginia, P.O. Box 3818, Charlottesville, VA 22903-0818.
[5] Department of Physics and Astronomy, The Johns Hopkins University, 3400 North Charles Street, Baltimore, MD 21218.
[6] Istituto Astrofisica Spaziale, CNR, Area di Tor Vergata, Via Fosso del Cavaliere 100, 00133 Rome, Italy.
[7] Istituto Astrofisica Spaziale, and Fisica Cosmica, CNR, Via Gobetti, 101, 40129 Bologna, Italy.
[8] Physics Department, University of Ferrara, Via Paradiso, 12, 44100 Ferrara, Italy.
[9] Columbia Astrophysics Laboratory, Columbia University, 550 West 120th Street, New York, NY 10027.
[10] Department of Astronomy, MSC 4500, New Mexico State University, P.O. Box 30001, Las Cruces, NM 88003.
[11] University of California at Berkeley, Space Sciences Laboratory, Berkeley, CA 94720-7450.
[12] Laboratory for Astronomy and Solar Physics, NASA Goddard Space Flight Center, Code 681, Greenbelt, MD 20771.
[13] Carnegie Observatories, 813 Santa Barbara Street, Pasadena, CA 91101.
[14] Center for Space Research, Massachusetts Institute of Technology, 70 Vassar Street, Cambridge, MA 02139-4307.
[15] Theoretical Astrophysics 130-33, California Institute of Technology, Pasadena, CA 91125.
[16] Astronomy Department, University of Texas, Austin, TX 78712.

Here we present optical and radio observations of GRB 020124, an afterglow that would have been classified as dark had it not been for rapid and deep searches. Furthermore, GRB 020124 is an example of an afterglow that is dim because of the combination of intrinsic faintness and a relatively fast decline, and not strong extinction.

2. OBSERVATIONS

2.1. *Ground-Based Observations*

GRB 020124, localized by the *HETE-2* satellite on 2002 January 24.44531 UT, had a duration of $\sim$70 s and a fluence (6–400 keV) of 3×10^{-6} ergs cm^{-2} (Ricker et al. 2002). Eight minutes after receiving the coordinates,[17] we observed the error box with the dual-band (B_M, R_M) MACHO imager mounted on the robotic 50 inch telescope at the Mount Stromlo Observatory (MSO). We also observed the error box with the Wide Field Imager on the 40 inch telescope at Siding Spring Observatory (SSO). We were unable to identify a transient source within the large error box (Price, Schmidt, & Axelrod 2002a).

We subsequently observed the error box refined by the Interplanetary Network (Hurley et al. 2002) with the Palomar 48 inch Oschin Schmidt using the unfiltered NEAT imager. Point-spread function (PSF)-matched image subtraction (Alard 2000) between the MACHO and NEAT images revealed a fading source (Price et al. 2002b), which was $R \approx 18$ mag at the epoch of our first observations and not present in the Digitized Sky Survey. Two nights later, we observed the afterglow using the Jacobs Camera (JCAM: Bloom 2002; Bloom et al. 2002b) mounted at the east arm focus of the Palomar 200 inch telescope (Bloom, Kulkarni, & Djorgovski 2002a). The position of the fading source is $\alpha(\mathrm{J2000.0}) = 9^{\mathrm{h}}32^{\mathrm{m}}50\overset{\mathrm{s}}{.}78$, $\delta(\mathrm{J2000.0}) = 11^{\circ}31'10\overset{''}{.}6$, with an uncertainty of about $0\overset{''}{.}4$ in each coordinate (Fig. 1).

[17] This corresponds to 1.6 hr after the burst detection.

TABLE 1
VLA Radio Observations of GRB 020124

Epoch (UT) (1)	ν_0 (GHz) (2)	Flux Density (μJy) (3)
Jan 26.22	8.46	84 ± 30
Jan 26.25	22.5	-60 ± 100
Jan 27.22	8.46	45 ± 25
Feb 1.40	8.46	49 ± 17
Jan 26.22–Feb 1.40	8.46	48 ± 13

Note.—Col. (1): UT date of each observation; col. (2): observing frequency; and col. (3): flux density at the position of the radio transient with the rms noise calculated from each image. The last row gives the flux density at 8.46 GHz from the co-added map.

Using the Very Large Array (VLA),[18] we observed the fading source at 8.46 and 22.5 GHz (see Table 1). We detect a faint source, possibly fading, at 8.46 GHz located at $\alpha(\mathrm{J2000.0}) = 9^{\mathrm{h}}32^{\mathrm{m}}50\overset{\mathrm{s}}{.}81$, $\delta(\mathrm{J2000.0}) = -11^{\circ}31'10\overset{''}{.}6$, with an uncertainty of about $0\overset{''}{.}1$ in each coordinate. Given the positional coincidence between the fading optical source and radio detection, we suggest that this source is the afterglow of GRB 020124.

The optical images were bias-subtracted and flat-fielded in the standard manner. To extract the photometry, we weighted the aperture with a Gaussian equivalent to the seeing disk ("weighted-aperture photometry"), using IRAF/*wphot*. The photometric zero points were set through photometry of calibrated field stars (Henden 2002) with

[18] The VLA is operated by the National Radio Astronomy Observatory, a facility of the National Science Foundation operated under cooperative agreement by Associated Universities, Inc.

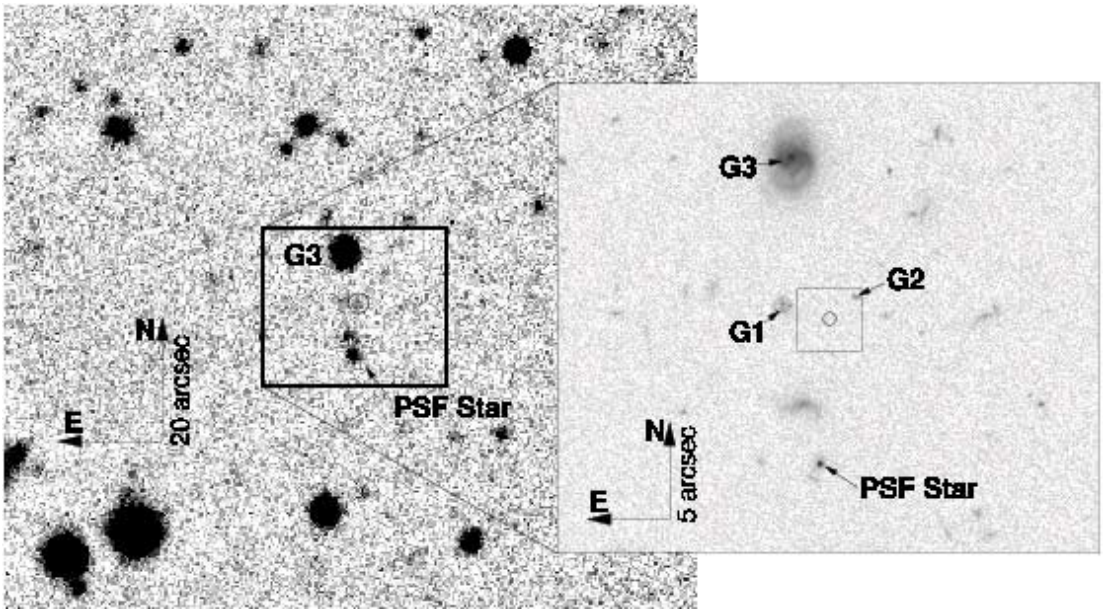

Fig. 1.—Palomar 200 inch (*left*) and *HST* epoch 1 (inset) images of the field of GRB 020124. The optical transient (OT) is circled in both images. The OT was of comparable brightness to G1 at the epoch of the Palomar 200 inch image and significantly fainter than G1 3 weeks later. The box overlaying the inset shows the portion of the *HST* images depicted in Fig. 2. Relevant sources described in the text are noted. The *HST* image is shown with logarithmic scaling to highlight the features of nearby galaxies.

TABLE 2
GROUND-BASED OPTICAL OBSERVATIONS OF GRB 020124

UT (1)	Telescope (2)	Band (3)	Magnitude (4)
Jan 24.51204	MSO 50	R_M	17.918 ± 0.041
Jan 24.51204	MSO 50	B_M	18.628 ± 0.057
Jan 24.51516	SSO 40	R	18.219 ± 0.046
Jan 24.51655	MSO 50	R_M	17.984 ± 0.044
Jan 24.51655	MSO 50	B_M	18.727 ± 0.063
Jan 24.51938	SSO 40	R	18.371 ± 0.091
Jan 24.52106	MSO 50	R_M	18.111 ± 0.049
Jan 24.52106	MSO 50	B_M	18.842 ± 0.069
Jan 24.52373	SSO 40	R	18.376 ± 0.082
Jan 24.55791	MSO 50	R_M	18.678 ± 0.048
Jan 24.55791	MSO 50	B_M	19.661 ± 0.090
Jan 24.56243	MSO 50	R_M	18.867 ± 0.036
Jan 24.56243	MSO 50	B_M	19.584 ± 0.053
Jan 24.56696	MSO 50	R_M	18.843 ± 0.039
Jan 24.56696	MSO 50	B_M	19.714 ± 0.050
Jan 26.34100	P 200	r'	24.398 ± 0.228

NOTE.—Col. (1): UT date of each observation; col. (2): telescope (MSO 50: Mount Stromlo Observatory 50 inch; SSO 40: Siding Spring Observatory 40 inch; P 200: Palomar Observatory 200 inch); col. (3): observing band; and col. (4): magnitudes and uncertainties. The observed magnitudes are not corrected for Galactic extinction.

magnitudes transformed to the appropriate system (Bessell & Germany 1999; Smith et al. 2002). The photometry is summarized in Table 2.

2.2. *Hubble Space Telescope Observations*

We observed the afterglow with the *Hubble Space Telescope* (*HST*) using the Space Telescope Imaging Spectrograph (STIS) on 2002 February 11.09, 18.30, and 25.71 UT (Bloom et al. 2002a), as part of our *HST* Cycle 10 program (GO-9180, PI: Kulkarni). The *HST* observations consisted of 750–850 s exposures. The *HST* data were retrieved after "on-the-fly" preprocessing. Using IRAF we drizzled (Fruchter & Hook 2002) each image onto a grid with pixels smaller than the original by a factor of 2 and using *pixfrac* of 0.7.

We found an astrometric tie between the *HST* and JCAM images using IRAF/*geomap* with nine suitable astrometric tie objects in common between the images. The rms of the resultant mapping is 133 mas (R.A.) and 124 mas (decl.). Using this mapping and IRAF/*geoxytrans*, we transferred the afterglow position on the JCAM image to the *HST* images. The rms of the transformation is 604 mas (R.A.) and 596 mas (decl.) and is dominated by the uncertainty in the JCAM position.

The source S1 (Fig. 2) coincides with the afterglow position within the astrometric uncertainty. We performed differential photometry at the position of S1 by registering the images of epochs 1 and 2 using a cross-correlation of a field of size $10''$ centered on S1 (using IRAF/*crosscor* and IRAF/*shiftfind*). We used IRAF/*center* and the FWHM of a relatively bright point source ("PSF star," Fig. 1) to fix the position of S1 in each of the final images and to determine the uncertainty in the position.

We photometered the source (and the PSF star) in epoch 1 using IRAF/*phot*, in a 3.4 pixel (86 mas) drizzled aperture radius. The small radius was chosen to maximize the signal-to-noise ratio of the detection of the faint point source, although, as found using the STIS instrument manual and confirmed with the PSF star, this radius encircles only $\sim$55% of the light of a point source. A corresponding correction was applied to the fluxes found in this aperature; we estimate a 0.1 mag systematic uncertainty due to this correction. Using IRAF/*synphot* and assuming a source spectrum of $f_\lambda \propto \lambda^{-0.5}$ (see below), we find that the source was $R = 28.68^{-0.20}_{+0.25}$ mag at the time of epoch 1. A bluer spectrum would result in an even fainter R-band magnitude, by as much as 0.25 mag for $f_\lambda \propto \lambda^{-2.5}$. More importantly, a redder spectrum would have little effect at the R band, with an increase of less than 0.05 mag. The photometry of the three epochs is summarized in Table 3. Note that this more careful analysis supersedes our preliminary report (Bloom 2002; Bloom et al. 2002c).

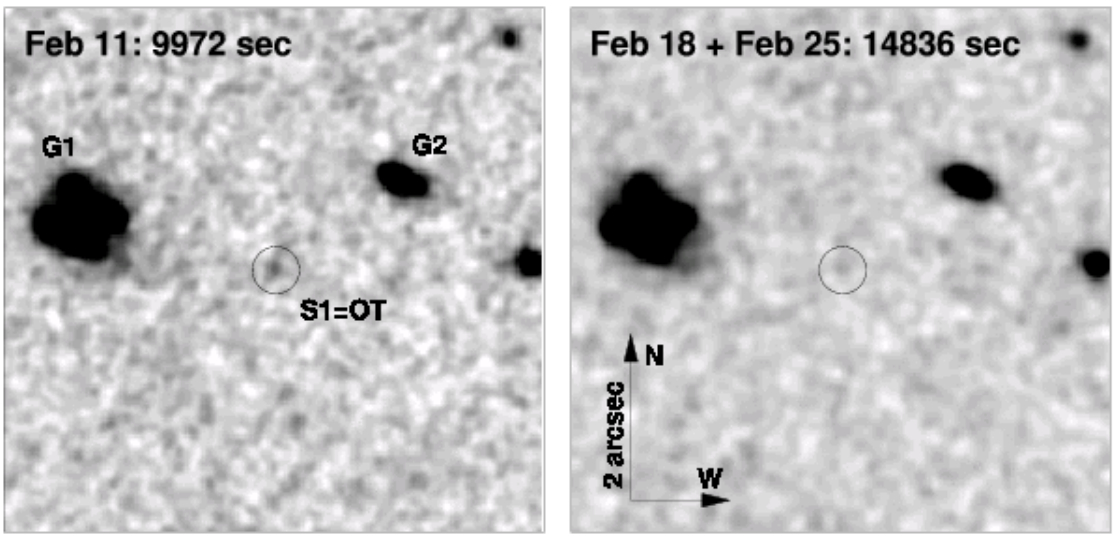

FIG. 2.—Faint OT of GRB 020124 as viewed using *HST*/STIS. Shown are (*left*) the summed, smoothed images from epoch 1 and (*right*) epochs 2+3. The gray scales have been matched such that a given flux is represented by the same shade in each image. The circle is centered at the same sky position in both images. Clearly, the source S1, identified with the position of the afterglow of GRB 020124, has faded.

TABLE 3
HST/STIS OBSERVATIONS OF GRB 020124

Epoch (UT) (1)	Band (2)	Exposure Time (ks) (3)	Flux ($e^- s^{-1}$) (4)	S/N (5)	Magnitude (6)
Feb 11.09	50 CCD/Clear	10.0	0.0814 ± 0.0169	4.82	$R = 28.68^{+0.25}_{-0.20}$
Feb 18.30	50 CCD/Clear	7.4	0.0443 ± 0.0189	2.34	$R = 29.35^{+0.60}_{-0.39}$
Feb 25.71	50 CCD/Clear	7.5	0.0362 ± 0.0183	1.98	$R = 29.56^{+0.76}_{-0.44}$
Feb 18.30+25.71	50 CCD/Clear	14.9	0.0398 ± 0.0137	2.91	$R = 29.46^{+0.46}_{-0.32}$

NOTE.—Col. (1): UT date of each observation; col. (2): STIS CCD mode; col. (3): exposure time; col. (4): flux and uncertainty; col. (5): significance; and col. (6): R magnitude and uncertainty. The total number of counts was converted to the R band, assuming the observed color of the OT, $f_\lambda \propto \lambda^{-0.5}$ (§ 2.2). The R-band errors reflect only the statistical uncertainty. Choosing a wide range of assumed colors for the afterglow ($\alpha_\lambda = -2.5$–0.5) gives $+0.25, -0.05$ mag. Thus, the afterglow could not have been much brighter in the R band than reported in epoch 1. We include this color uncertainty in the analysis (§ 3), and in Fig. 3, choosing half of the range as the rms of the systematic color uncertainty. In addition, we also include in the analysis the estimated uncertainty from the aperture correction (0.1 mag; § 2.2). For epochs 2 and 3, the 3 σ upper limits are $R = 29.09$ and 29.13 mag, respectively. The observed magnitudes are not corrected for Galactic extinction.

There are no obvious persistent sources within 1.″75 of the optical transient (OT) down to $R \approx 29.5$ mag. To date, all of the GRBs localized to subarcsecond accuracy have viable hosts brighter than this level within $\sim$1.″3 of the OT position (Bloom 2002; Bloom et al. 2002a). The faintest host to date is that of GRB 990510, $R \sim 28.5$ mag ($z = 1.619$; Vreeswijk et al. 2001). Thus, the host of GRB 020124 may be at a somewhat higher redshift; however, $z \lesssim 4.5$, since the afterglow was detected in the B_M filter.

3. MODELING OF THE OPTICAL DATA

In Figure 3 we plot the optical light curves of GRB 020124, including a correction for Galactic extinction, $E(B-V) = 0.052$ mag (Schlegel et al. 1998). The optical light curves are usually modeled as $F_\nu(t,\nu) = F_{\nu,0}(t/t_0)^\alpha(\nu/\nu_0)^\beta$. However, as can be seen in Figure 3, the

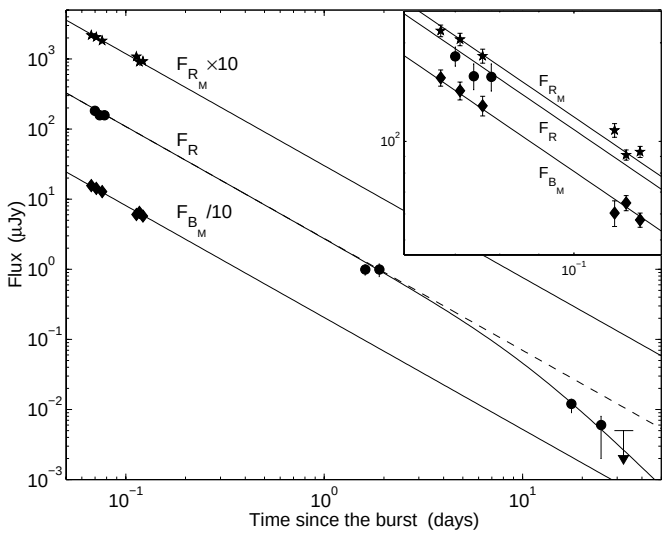

FIG. 3.—Optical light curves of GRB 020124 (*top to bottom*: R_M, R, and B_M), corrected for Galactic extinction, $E(B-V) = 0.052$ mag (Schlegel et al. 1998). The solid lines are a representative jet model (ISM/Wind$_R$, see Table 4), while the dashed line is an extrapolation of the early evolution without a break. With no break in the R-band light curve, the predicted magnitude at the epoch of the first *HST* observation exceeds the measured values by 5 σ. The flux measured in the last *HST* epoch is plotted as a 2 σ upper limit.

R-band light curve cannot be described by a single power law. Restricting the fit to $t < 2$ days, we obtain ($\chi^2_{\rm min} = 15$ for 14 degrees of freedom), $\alpha_1 = -1.60 \pm 0.04$, $\beta = -1.43 \pm 0.14$, and $F_{\nu,0} = 2.96 \pm 0.25$ μJy; here, $F_{\nu,0}$ is defined at the effective frequency of the R_M filter, and $t = 1$ day. For $t > 2$ days, we get $\alpha_2 = -1.9^{+1.0}_{-2.0}$. The uncertainty in α_2 is large because it is effectively constrained by only two data points. However, if we make the additional requirement that the fits to the ground-based data and the *HST* data intersect at $t > 2$ days, we find that $\alpha_2 = -1.9^{+0.1}_{-2.0}$, and the steepening is therefore significant at the 2.5 σ level.

To account for the steepening, we modify the model for the R-band light curve to

$$F_\nu(t,\nu) = F_{\nu,0}(\nu/\nu_0)^\beta \left[(t/t_b)^{\alpha_1 n} + (t/t_b)^{\alpha_2 n}\right]^{1/n}, \quad (1)$$

where α_1 is the asymptotic index for $t \ll t_b$, α_2 is the asymptotic index for $t \gg t_b$, $n < 0$ provides a smooth joining of the two asymptotic segments, and t_b is the time at which the asymptotic segments intersect. We retain the simple model for the R_M and B_M light curves, since they are restricted to $t \lesssim 0.13$ days (i.e., well before the observed steepening).

We investigate two alternatives for the observed steepening in the framework of the afterglow synchrotron model (e.g., Sari, Piran, & Narayan 1998), namely, (1) a cooling break (§ 3.1) and (2) a jet break (§ 3.2). In this framework, α_1, α_2, and β are related to each other through the index (p) of the electron energy distribution, $N(\gamma) \propto \gamma^{-p}$ (for $\gamma > \gamma_{\rm min}$). The relations for the models discussed below, as well as the resulting closure relations, $\alpha_1 + b\beta + c = 0$, are summarized in Table 4.

3.1. *Cooling Break*

The observed steepening, $\Delta\alpha \equiv \alpha_2 - \alpha_1 \approx -0.3$, can be due to the passage of the synchrotron cooling frequency, ν_c, through the R band.[19] This has been suggested, for example, in the afterglow of GRB 971214, at $t \sim 0.6$ days (Wijers & Galama 1999). If the steepening is due to ν_c, this rules out

[19] We note that while the passage of ν_c through the R band will also change the spectrum of the afterglow by $\delta\beta = -0.5$ (i.e., the afterglow would become somewhat redder), this has little effect on the conversion of the STIS count rate to R-band magnitudes (see § 2.2). We therefore use the same source magnitudes listed in Table 3, along with the relevant systematic uncertainties.

TABLE 4
AFTERGLOW MODELS

Model (1)	α_1 (2)	α_2 (3)	β (4)	(b, c) (5)	Closure (6)	p (7)	$A_V^{\rm host}$ (mag) (8)
ISM_B	$-3(p-1)/4$	$-(3p/4)+1/2$	$-(p-1)/2$	$(-3/2, 0)$	0.52 ± 0.28	3.17 ± 0.05	(0.35, 0.18, 0.10)
Jet_B	$-p$	$-p$	$-(p-1)/2$	$(-2, 1)$	2.23 ± 0.36	1.63 ± 0.04	(0.89, 0.50, 0.22)
$\mathrm{J\text{-}ISM}_B$.....	$-3(p-1)/4$	$-p$	$-(p-1)/2$	$(-3/2, 0)$	0.52 ± 0.28	3.17 ± 0.05	(0.30, 0.10, 0.05)
$\mathrm{J\text{-}Wind}_B$	$-(3p-1)/4$	$-p$	$-(p-1)/2$	$(-3/2, 1/2)$	1.02 ± 0.28	2.51 ± 0.05	(0.30, 0.16, 0.08)
$\mathrm{J\text{-}ISM/Wind}_R$.....	$-(3p-2)/4$	$-p$	$-p/2$	$(-3/2, -1/2)$	0.02 ± 0.28	2.84 ± 0.05	...

NOTE.—Col. (1): Afterglow model (ISM: r^0 circumburst medium; Wind: r^{-2} circumburst medium; Jet: collimated eject with opening angle $\theta_{\rm jet}$; a subscript B indicates $\nu_c < \nu_{\rm opt}$, and a subscript R indicates $\nu_c > \nu_{\rm opt}$); col. (2): α_1 as a function of p; col. (3): α_2 as a function of p; col. (4): β as a function of p; col. (5): closure relations ($\alpha + b\beta + c = 0$); col. (6): resulting closure values from the observed values of α_1 and β; col. (7): inferred value of p from the measured value of α_1; and col. (8): the required extinction in the frame of the host galaxy for closure values of zero ($z = 0.3, 1, 3$); typical uncertainties are ± 0.05 mag. The top two models apply to the case when the observed steepening in the light curves is due to the passage of ν_c through the R-band, while the bottom three apply to the case when the steepening is due to a jet.

models in which the ejecta expand into a circumburst medium with $\rho \propto r^{-2}$ (hereafter Wind), because in this model ν_c increases with time ($\propto t^{1/2}$; Chevalier & Li 1999), and one expects $\Delta\alpha = 0.25$.

There are two remaining models to consider in this case: (1) spherical expansion into a circumburst medium with constant density (hereafter ISM_B; Sari et al. 1998), and (2) a jet with $\theta_{\rm jet} < \Gamma^{-1}_{t\sim 0.06\ \rm days}$ (i.e., a jet break prior to the first observation at $t \approx 0.06$ days; hereafter Jet_B). The subscript B indicates that ν_c is blueward of the optical bands initially. In both models we use equation (1) for the R-band light curve, with t_b defined as the time at which $\nu_c = \nu_R$, and $\alpha_2 \equiv \alpha_1 - 1/4$.

We find that in the ISM_B model $t_c \approx 0.4$ days, while in the Jet_B model $t_c \approx 0.65$ days. Moreover, in both models the closure relations can only be satisfied by including a contribution from dust extinction within the host galaxy, $A_V^{\rm host}$. We estimate the required extinction using the parametric extinction curves of Cardelli, Clayton, & Mathis (1989) and Fitzpatrick & Massa (1988), along with the interpolation calculated by Reichart (2001). Since the redshift of GRB 020124 is not known, we assume $z = 0.3, 1,$ and 3, which spans the range of typical redshifts for the long-duration GRBs. The inferred values of $A_V^{\rm host}$ are summarized in Table 4, and range from 0.2 to 0.9 mag.

3.2. *Jet Break*

An alternative explanation for the steepening is a jet expanding into (1) an interstellar medium (ISM) with ν_c blueward of the optical bands ($\mathrm{J\text{-}ISM}_B$), (2) a Wind medium with ν_c blueward of the optical bands ($\mathrm{J\text{-}Wind}_B$), and (3) an ISM or Wind medium with ν_c redward of the optical bands ($\mathrm{J\text{-}ISM/Wind}_R$). We note that the $\mathrm{J\text{-}ISM}_B$ model is different from the ISM_B model (§ 3.1), since previously it was implicitly defined such that the jet break is later than the last observation. In these models, $t_b \equiv t_{\rm jet}$ is the time at which $\Gamma(t_{\rm jet}) \approx \theta_{\rm jet}^{-1}$.

From the closure values, we note that the $\mathrm{J\text{-}ISM/Wind}_R$ requires no extinction within the host galaxy, while the $\mathrm{J\text{-}ISM}_B$ and $\mathrm{J\text{-}Wind}_B$ models require values of about 0.05–0.3 mag.

We find $t_{\rm jet} \sim 10$–20 days, corresponding to $\theta_{\rm jet} \sim 10^\circ$. Using the measured fluence (§ 2.1), we estimate the beaming-corrected gamma-ray energy, $E_\gamma \approx 5 \times 10^{50}\ n_1^{1/4}$ ergs, assuming a circumburst density $n_1 = 1\ \mathrm{cm}^{-3}$ and $z = 1$ (E_γ is a weak function of z). This value is in good agreement with the distribution of E_γ for long-duration GRBs (Frail et al. 2001).

4. DISCUSSION AND CONCLUSIONS

Regardless of the specific model for the afterglow emission, the main conclusion of § 3 is that the optical afterglow of GRB 020124 suffered little or no dust extinction. Still, this afterglow would have been missed by typical searches undertaken even as early as 12 hr after the GRB event. As shown in Figure 4 and Table 5, about 70% of the searches conducted to date would have failed to detect an optical afterglow like that of GRB 020124.

This is simply because the afterglow of GRB 020124 was faint and exhibited relatively rapid decay. From Figure 5 we note that GRB 020124 is one of the faintest afterglows detected to date (normalized to $t = 1$ day), and while it is

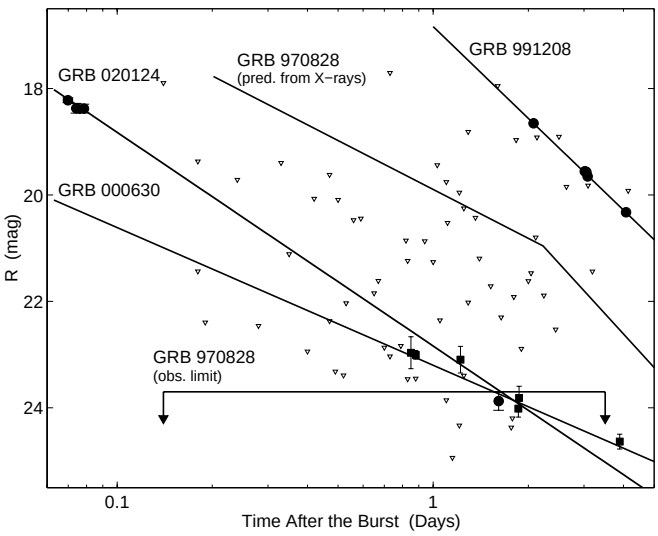

FIG. 4.—R-band upper limits from searches of well-localized GRBs, corrected for Galactic extinction. The limits up to GRB 000630 are taken from Fynbo et al. (2001), while subsequent limits are from the GRB Coordinates Network. Also shown are the light curves of the GRB 020124, GRB 000630, the bright GRB 991208 (Castro-Tirado et al. 2001), and GRB 970828 (the dereddened light curve is based on the radio and X-ray data; Djorgovski et al. 2001a). Only about 30% of the searches yielded limits that are fainter than the afterglow of GRB 020124. A similar fraction was found by Fynbo et al. (2001) based on the afterglow of GRB 000630.

TABLE 5
LIMITS ON OPTICAL AFTERGLOW MAGNITUDES

GRB (1)	Epoch (days) (2)	*R* Limit (mag) (3)	Reference (4)
GRB 000801	1.77	24.5	GCN 767
GRB 000812	4.14	20.8	GCN 771
GRB 000830	0.99	24.5	GCN 788
GRB 001025	1.21	24.5	GCN 867
GRB 001204	3.09	20.1	GCN 898
GRB 010103	1.83	19.2	GCN 911
GRB 010119	1.13	18	GCN 919
GRB 010126	0.88	23.5	GCN 926
GRB 010214	0.83	21.3	GCN 949
GRB 010220	0.35	23.5	GCN 958
GRB 010324	1.29	22.3[a]	GCN 1024
GRB 010326A	0.50	21.5	GCN 1022
GRB 010412	0.60	20.5[a]	GCN 1039
GRB 011019	1.15	25.0	GCN 1128
GRB 011212	2.0	24.0	GCN 1324
GRB 020127	0.18	19.5	GCN 1230
GRB 020409	1.25	23.5	GCN 1362

NOTE.—Col. (1): GRB name; col. (2): observing time after the burst; col. (3): *R*-band limit; and col. (4): GCN circular reference.
[a] *V*-band limit.

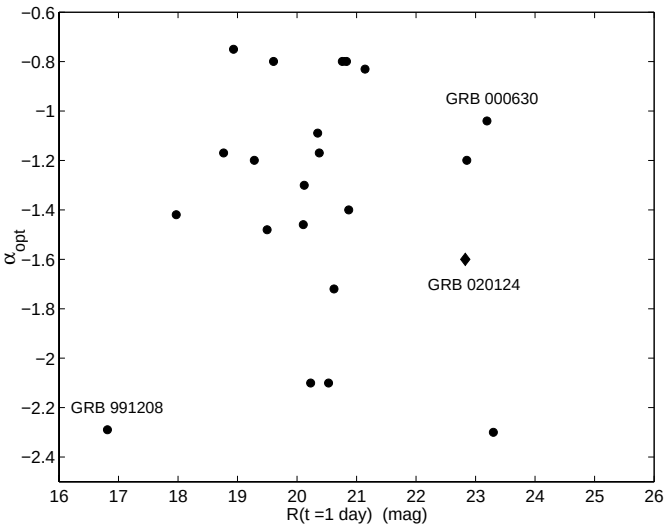

FIG. 5.—Temporal decay index, α_{opt} ($F_\nu \propto t^\alpha$), plotted against the *R*-band magnitude at $t = 1$ day for several optical afterglows. We chose a fiducial time of 1 day, since, with the exception of GRB 010222, all the observations are before the jet break. While the majority of optical afterglows cluster around $R(t = 1 \text{ day}) \sim 20$ mag, GRB 020124 is one of the four faintest afterglows detected to date, and one of the six most rapid faders.

not an excessively rapid fader, it is in the top 30% in this category.

Thus, the afterglow of GRB 020124, along with that of GRB 000630 (Fynbo et al. 2001; Fig. 5) and GRB 980613 (Hjorth et al. 2002), indicates that there is a wide diversity in the brightness and decay rates of optical afterglows. In fact, the brightness distribution spans a factor of about 400, while the decay index varies by more than a factor of 3. Coupled with the low dust extinction in the afterglow of GRB 020124, this indicates that some dark bursts may simply be dim, and not dust-obscured.

Given this wide diversity in the brightness of optical afterglows, it is important to establish directly that an afterglow is dust obscured. This has only been done in a few cases (§ 1). Therefore, while *statistical* analyses (e.g., Reichart & Yost 2001) point to extinction as the underlying reason for some fraction of dark bursts, it is clear that observationally, the issue of dark bursts is not settled, and the observational biases have not been traced fully (see also Fynbo et al. 2001).

Since progress in our understanding of dark bursts will benefit from observations, we need consistent, rapid follow-up of a large number of bursts to constrain the underlying distribution, as well as complementary techniques that can directly measure material along the line of sight. This includes X-ray observations that allow us to measure the column density to the burst (Galama & Wijers 2001) and thus infer the type of environment and potential extinction level. Along the same line, radio observations allow us to infer the synchrotron self-absorption frequency, which is sensitive to the ambient density (e.g., Sari & Esin 2001); the detection of radio emission, as in the case of GRB 020124, implies a density $n \lesssim 10^2$ cm^{-3}. Finally, prompt optical observations, as we have carried out in this case, may uncover a larger fraction of the dim optical afterglows and provide a better constraint on the fraction of truly obscured bursts.

J. S. B. is a Fannie and John Hertz Foundation Fellow. F. A. H. acknowledges support from a Presidential Early Career award. S. R. K. and S. G. D. thank the NSF for support. R. S. is grateful for support from a NASA ATP grant. R. S. and T. J. G. acknowledge support from the Sherman Fairchild Foundation. J. C. W. acknowledges support from NASA grant NAG 59302. K. H. is grateful for *Ulysses* support under JPL contract 958056 and for IPN support under NASA grants FDNAG 5-11451 and NAG 5-17100. Support for Proposal HST-GO-09180.01-A was provided by NASA through a grant from the Space Telescope Science Institute, which is operated by the Association of Universities for Research in Astronomy, Inc., under NASA contract NAS5-26555. We thank the anonymous referee for helpful comments.

REFERENCES

Alard, C. 2000, A&AS, 144, 363
Bessel, M. S., & Germany, L. M. 1999, PASP, 111, 1421
Bloom, J. S. 2002, GCN Circ. 1225
Bloom, J. S., Kulkarni, S. R., & Djorgovski, S. G. 2002a, AJ, 123, 1111
Bloom, J. S., et al. 2002b, PASP, submitted
———. 2002c, GCN Circ. 1389
Cardelli, J. A., Clayton, G. C., & Mathis, J. S. 1989, ApJ, 345, 245
Castro-Tirado, A. J., et al. 2001, A&A, 370, 398
Chevalier, R. A., & Li, Z.-Y. 1999, ApJ, 520, L29
Djorgovski, S. G., et al. 2001a, ApJ, 562, 654
Djorgovski, S. G., et al. 2001b, in Proc. ESO Astrophysics Symposia, Gamma-Ray Bursts in the Afterglow Era: 2nd Workshop, ed. E. Costa, F. Frontera, & J. Hjorth (Berlin: Springer), 218
Fitzpatrick, E. L., & Massa, D. 1988, ApJ, 328, 734
Frail, D. A., et al. 2001, ApJ, 562, L55
Fruchter, A. S., & Hook, R. N. 2002, PASP, 114, 144
Fynbo, J. U., et al. 2001, A&A, 369, 373
Galama, T. J., & Wijers, R. A. M. J. 2001, ApJ, 549, L209
Groot, P. J., et al. 1998, ApJ, 502, L123
Henden, A. 2002, GCN Circ. 1251

Hjorth, J., et al. 2002, ApJ, 576, 113
Hurley, K. H., et al. 2002, GCN Circ. 1223
Kulkarni, S. R., et al. 2000, Proc. SPIE, 4005, 9
Lazzati, D., Covino, S., & Ghisellini, G. 2002, MNRAS, 330, 583
Piro, L., et al. 2002, ApJ, 577, 680
Price, P. A., Schmidt, B. P., & Axelrod, T. S. 2002a, GCN Circ. 1219
Price, P. A., et al. 2002b, GCN Circ. 1221
Ramirez-Ruiz, E., Trentham, N., & Blain, A. W. 2002, MNRAS, 329, 465
Reichart, D. E. 2001, ApJ, 553, 235
Reichart, D. E., & Price, P. A. 2002, ApJ, 565, 174
Reichart, D. E., & Yost, S. 2001, ApJ, submitted (astro-ph/0107545)
Ricker, G., et al. 2002, GCN Circ. 1220
Sari, R., & Esin, A. A. 2001, ApJ, 548, 787
Sari, R., Piran, T., & Narayan, R. 1998, ApJ, 497, L17
Schlegel, D., et al. 1998, ApJ, 500, 525
Smith, J. A., et al. 2002, AJ, 123, 2121
Taylor, G. B., et al. 2000, ApJ, 537, L17
Vreeswijk, P. M., et al. 2001, ApJ, 546, 672
Wijers, R. A. M. J., & Galama, T. J. 1999, ApJ, 523, 177